STEM CELLS TRANSLATIONAL MEDICINE®

FETAL AND NEONATAL STEM CELLS

Human Cardiomyocytes Prior to Birth by Integration-Free Reprogramming of Amniotic Fluid Cells

GUIHUA JIANG,[a,b] TODD J. HERRON,[c] JULIE DI BERNARDO,[a] KENDAL A. WALKER,[a,b] K. SUE O'SHEA,[b,d] SHAUN M. KUNISAKI[a,b,e]

Key Words. Cardiac • Fetal stem cells • Pluripotent stem cells • Induced pluripotent stem cells • Amniotic fluid

[a]Department of Surgery, [b]Pluripotent Stem Cell Laboratory, [c]Department of Internal Medicine, Cardiovascular Research Center, [d]Department of Cell and Developmental Biology, and [e]C.S. Mott Children's Hospital and Von Voigtlander Women's Hospital, University of Michigan Medical School, Ann Arbor, Michigan, USA

Correspondence: Shaun M. Kunisaki, M.D., C.S. Mott Children's Hospital and Von Voigtlander Women's Hospital, 1540 East Hospital Drive, SPC 4211, Ann Arbor, Michigan 48109, USA. Telephone: 734-936-8464; E-Mail: shaunkun@umich.edu

Received January 11, 2016; accepted for publication June 13, 2016; published Online First on July 27, 2016.

1066-5099/2016/$20.00/0

http://dx.doi.org/10.5966/sctm.2016-0016

ABSTRACT

The establishment of an abundant source of autologous cardiac progenitor cells would represent a major advance toward eventual clinical translation of regenerative medicine strategies in children with prenatally diagnosed congenital heart disease. In support of this concept, we sought to examine whether functional, transgene-free human cardiomyocytes (CMs) with potential for patient-specific and autologous applications could be reliably generated following routine amniocentesis. Under institutional review board approval, amniotic fluid specimens (8–10 ml) at 20 weeks gestation were expanded and reprogrammed toward pluripotency using nonintegrating Sendai virus (SeV) expressing *OCT4, SOX2, cMYC,* and *KLF4*. Following exposure of these induced pluripotent stem cells to cardiogenic differentiation conditions, spontaneously beating amniotic fluid-derived cardiomyocytes (AF-CMs) were successfully generated with high efficiency. After 6 weeks, quantitative gene expression revealed a mixed population of differentiated atrial, ventricular, and nodal AF-CMs, as demonstrated by upregulation of multiple cardiac markers, including *MYH6, MYL7, TNNT2, TTN,* and *HCN4*, which were comparable to levels expressed by neonatal dermal fibroblast-derived CM controls. AF-CMs had a normal karyotype and demonstrated loss of *NANOG, OCT4*, and the SeV transgene. Functional characterization of SIRPA$^+$ AF-CMs showed a higher spontaneous beat frequency in comparison with dermal fibroblast controls but revealed normal calcium transients and appropriate chronotropic responses after β-adrenergic agonist stimulation. Taken together, these data suggest that somatic cells present within human amniotic fluid can be used to generate a highly scalable source of functional, transgene-free, autologous CMs before a child is born. This approach may be ideally suited for patients with prenatally diagnosed cardiac anomalies. STEM CELLS TRANSLATIONAL MEDICINE *2016;5:1595–1606*

SIGNIFICANCE

This study presents transgene-free human amniotic fluid-derived cardiomyocytes (AF-CMs) for potential therapy in tissue engineering and regenerative medicine applications. Using 8–10 ml of amniotic fluid harvested at 20 weeks gestation from normal pregnancies, a mixed population of atrial, ventricular, and nodal AF-CMs were reliably generated after Sendai virus reprogramming toward pluripotency. Functional characterization of purified populations of beating AF-CMs revealed normal calcium transients and appropriate chronotropic responses after β-adrenergic agonist stimulation in comparison with dermal fibroblast controls. Because AF-CMs can be generated in fewer than 16 weeks, this approach may be ideally suited for eventual clinical translation at birth in children with prenatally diagnosed cardiac anomalies.

INTRODUCTION

Congenital heart defects (CHD) are the most common type of birth defect in the United States, affecting nearly 1% of births per year [1]. Almost half of these cases are now diagnosed prenatally by ultrasound [2]. Many of these children will ultimately require major heart surgery or other invasive procedures as infants, and approximately 25% will die before 1 year of age under conventional medical and surgical treatment [1, 3]. There remains a critical need for new technologies to better understand the pathogenesis of CHD and to develop novel therapeutic approaches that can improve the lives of these children and their families.

The reliable generation of patient-specific cardiomyocytes (CMs) from induced pluripotent stem cells (iPSCs) before a child is even born is a relatively novel regenerative medicine strategy that might bring new hope in CHD [4, 5]. Cardiac anomalies are composed of a heterogeneous group of conditions for which few suitable animal

models exist [6]. Patient-specific CMs could therefore provide a useful in vitro model to study disease pathogenesis. Moreover, the generation of autologous CMs using nonintegrating techniques would provide new avenues for the development of cardiac cell-based therapies and three-dimensional (3D) engineered microtissues aimed at treating heart failure, either prenatally or in the early postnatal period, as an alternative to cadaveric heart transplantation.

In this study, we hypothesized that functional, transgene-free CMs with potential for patient-specific and autologous perinatal applications could be reliably generated in a minimally invasive fashion from somatic cells normally obtained by routine amniocentesis. For the first time, we show the successful generation of functional, transgene-free CMs derived from fetal amniotic fluid iPSCs in normal patients. These CMs were subsequently compared with CMs derived from postnatal dermal fibroblasts. We further demonstrate that human CMs generated from amniotic fluid have similar phenotypic and functional properties in comparison with fibroblast-derived controls and may therefore be ideally suited for cardiac regenerative therapies in fetuses and neonates with prenatally diagnosed cardiac anomalies.

Materials and Methods

Human Specimens

Approval for this work was obtained from the University of Michigan (IRB 38565 and HPSCRO 1044). After written informed consent, human somatic cells were obtained from normal 20-week gestation unused amniocentesis samples (n = 2, 8–10 ml) performed for obstetrical indications. Specimen donations were anonymous and would have otherwise been discarded as waste. As controls, neonatal foreskin specimens (n = 2) were obtained following elective circumcision. All patients were confirmed to have normal heart function postnatally. After 24–48 hours, nonadherent cells were removed by washing the plates with phosphate-buffered saline, and the medium was replaced as previously described [7].

Somatic Cell Characterization

Between passages 3 and 5, skin dermal fibroblasts and amniocytes were phenotypically characterized for pluripotency and mesenchymal stem cell (MSC) features on the basis of criteria as described elsewhere [8]. Differentiation into mesenchymal lineages was performed at passage 4, as detailed elsewhere [9]. For flow cytometry, primary antibodies used were phycoerythron-conjugated against CD34, CD44, CD45, CD73, CD90, CD105, CD117 (c-kit), *OCT4A, SOX2*, SSEA3, SSEA4, TRA-1-60, TRA-1-81, and human leukocyte antigen-antigen D related (HLA-DR) (all from BD Biosciences, San Diego, CA, http://www.bdbiosciences.com). Cells were fixed with 2% paraformaldehyde prior to evaluation of antibody staining using a LSRII flow cytometer (BD Biosciences). Resulting data were analyzed using FloJo software (Tree Star, Ashland, OR, http://www.flowjo.com).

iPSC Derivation

Integration-free iPSC derivation was performed using a nonintegrating, cytoplasmic Sendai virus (SeV) encoding for *OCT4, SOX2, KLF4*, and *cMYC* (OSKM) at 3×10^6 cell infectious units (CytoTune-iPS Reprogramming Kit, Thermo Fisher Scientific Life Sciences, Waltham, MA, https://www.thermofisher.com), as previously described in our laboratory [10]. Briefly, 2×10^5 amniotic fluid mesenchymal stromal cells (AF-MSCs) or dermal fibroblasts were exposed to SeV for 24 hours and subsequently placed on irradiated mouse embryonic fibroblast (MEFs) feeder layers. All cells, including H1- and H9- human embryonic stem cell (ESC) controls (WiCell, Madison, WI, http://www.wicell.org), were cultured in human embryonic stem cell conditioned medium (GlobalStem, Gaithersburg, MD, http://www.globalstem.com) with 4 ng/ml of FGF-2 (Millipore, Damstadt, Germany, http://www.emdmillipore.com). Individual colonies were subsequently picked mechanically and propagated on MEFs or Matrigel (BD Biosciences).

Alkaline phosphatase (AP) staining was performed using the AP substrate kit (Millipore), according to the manufacturer's instructions. Immunofluorescence staining was used to assay pluripotency in established iPSC lines. Primary antibodies against *NANOG* (Abcam, Cambridge, MA, http://www.abcam.com), *OCT4* (Santa Cruz Biotechnology, Dallas, TX, http://www.scbt.com), *SOX2*, SSEA3, SSEA4, TRA-1-60, and TRA-1-81 (Millipore) were used. Cells were examined using epifluorescence microscopy (DM IRB, Leica, Buffalo Grove, IL, http://www.leica-microsystem.com). Karyotyping was performed on iPSCs by Cell Line Genetics (Madison, WI, http://www.clgenetics.com).

Embryoid Body Assay

Embryoid bodies (EBs) were formed in suspension culture and analyzed using methods previously described [11]. Primary antibodies were against neuron-specific class β-III tubulin (TuJ1; Covance, Battle Creek, MI, http://www.covance.com), *SOX17* (R&D Systems, Minneapolis, MN, http://www.rndsystems.com), and α-smooth muscle actin (SMA).

Cardiomyocyte Differentiation

iPSC clones (two per experiment) at passages 10 to 14 were incubated with TrypleE (Invitrogen) at 37°C for 5 minutes to obtain a single cell suspension. CM differentiation of iPSCs was performed using one of two established monolayer differentiation protocols in our laboratory. In the first approach, we used modifications of the Matrigel sandwich technique, as previously detailed [12]. We seeded 30,000 cells onto silicone membranes within Matrigel-coated 12-well plates in mTESR1 medium (StemCell Technologies, Vancouver, British Columbia, Canada, http://www.stemcell.com) and grew them to 80%–90% confluence, at which time the wells were overlaid with 1 ml Matrigel per well. Once the cells were 100% confluent, the medium was replaced with Roswell Park Memorial Institute (RPMI) 1640 (Invitrogen) containing B27 without insulin (Invitrogen), 100 ng/ml activin A (R&D Systems), and Matrigel. After 24 hours, the media were supplemented with 10 ng/ml BMP4 (R&D Systems) and 10 ng/ml FGF-2 (Millipore) for another 4 days prior to changing to basal media containing B27 with insulin (Invitrogen) for up to 90 days. In the small-molecule cardiac induction protocol as described elsewhere [13], the media on day 0 were replaced with RPMI 1640 containing B27 without insulin and 12 μM glycogen synthase kinase 3B inhibitor (CHIR99021, Selleck, Houston, TX, http://www.selleckchem.com) for 24 hours to activate canonical Wnt signaling. On day 3, the media were supplemented with 5 μM porcupine palmitylation inhibitor (IWP-4, Stemgent, Cambridge, MA, http://www.stemgent.com) for 24 hours to inhibit Wnt

signaling. The media were then changed to basal media containing B27 with insulin for up to 90 days.

Cardiomyocyte Separation

For all functional testing, enrichment for stem cell-derived CMs was performed on the basis of positive expression of signal regulatory protein α (SIRPA, CD172a; Miltenyi Biotec, San Diego, CA, http://www.miltenyibiotec.com) expression, as detailed elsewhere [14]. Briefly, CMs between 30 and 40 days were dissociated with 0.25% tryspin-EDTA at 37°C for 5 minutes and neutralized in EB20 medium. Cells were then incubated with antibiotin magnetic microbeads conjugated with SIRPA antibody at 4°C for 10 minutes and positively selected by passing the cell suspension through magnetic columns on a magnetic separator (Miltenyi Biotec). We seeded 300,000 cells onto silicone membranes coated with Matrigel in EB20 medium in 12-well plates. The media were replaced after 48 hours with RPMI 1640 plus B27 in preparation for electrophysiologic testing 1 week later. Assessment of CM purification was performed by flow cytometry using a cardiac troponin (cTnT) antibody (Miltenyi Biotec).

Gene Expression Analysis

Total RNA was extracted from cells using TRIzol (Invitrogen). First-strand cDNA was prepared with the Taqman Reverse Transcription Reagent kit (Applied Biosystems, c). Reverse transcription polymerase chain reaction (RT-PCR) was performed in triplicate at 35 cycles. The primer sequences for RT-PCR can be found in supplemental online Table 1. Quantitative PCR (qPCR) was carried out on a Mastercycler ep realplex (Eppendorf, Hamburg, Germany, http://www.eppendorf.com) using Fast SYBR Green Master Mix (Applied Biosystems), as recommended by the manufacturer. Relative gene expression of cardiac-specific myofilament and pluripotency transcripts was analyzed by qPCR with *GAPDH* used as a reference gene to normalize target gene expression using the $2^{-\Delta\Delta Ct}$ method [15]. The primer sequences used for qPCR are provided in supplemental online Table 2.

Microarray Analysis

To compare transcriptomes among the different cell types, we performed a customized microarray analysis of 88 genes on the basis of the Cardiovascular Disease PCR array kit (PAHS-174Z, QIAGEN, Valencia, CA, http://www.sabiosciences.com). A list of genes is shown in supplemental online Tables 3 and 4. Total RNA was extracted using the MagMAX-96 Total RNA Isolation Kit and MAG Max Express (Applied Biosystems) from randomly selected parental, iPSC, and $SIRPA^+$ CMs. RNA quality and quantity were determined spectrophotometrically using Nano Drop 2000 (Thermo Fisher, Waltham, MA, https://www.thermofisher.com). Sample processing, probing to the Human Gene 2.1 ST array platform (Affymetrix, Santa Clara, CA, http://www.affymetrix.com), and data analysis were performed by the University of Michigan DNA Sequencing Core Microarray Facility. Normalized expressions by robust multiple-array averages were plotted using the heatmap.2 function from the gplots package in R (http://www.r-project.org) using default parameters. The Euclidean distance dissimilarity matrix and complete linkage method were used to generate dendrograms and heatmap images. After exclusion of genes that were not present, we normalized values (in relation to housekeeping genes) on the basis of a 0-to-25 scale, with high expression shown in red and low expression shown in yellow.

Immunocytochemistry

For immunofluorescence analysis of cell type restricted proteins, cells were fixed in 4% paraformaldehyde and stained with primary antibodies against α-actinin (Sigma-Aldrich, St. Louis, MO, www.sigma-aldrich.com), myosin heavy chains (MF20 and *MYH7*), MLC2v (Proteintech, Chicago, IL, http://www.ptglab.com), or connexin-43 (CX43). Cells were counterstained with 4',6-diamidino-2-phenylindole (DAPI). Confocal imaging was performed by using a Zeiss LSM 510 and Nikon A-1 confocal system. Cell size was measured using the NIS-Elements (Nikon, Tokyo, Japan, www.nikonusa.com) software package. Four randomly selected cells per high power field were outlined, and cell size was calculated on the basis of microns per pixel.

GFP Labeling

Reporter constructs for the MLC2v and MLC2a promoters in the pAcGFP1-1 vector were used to generate recombinant adenoviruses as detailed elsewhere [16]. Viral infections of iPSC-CMs were performed at a multiplicity of infection of 100. Plates were placed into the IncuCyte incubator (Essen Bioscience, Ann Arbor, MI, http://www.essenbioscience.com) and monitored for cell growth for 60 hours.

Calcium Transients and Optical Mapping Studies

iPSC-CM monolayers in 12-well plates were loaded with Rhod-2, AM (5 μmol/l, Molecular Probes, Thermo Fisher) for 10 minutes to monitor intracellular calcium flux and wave propagation using a previously described LED illumination optical mapping system [17, 18]. A bipolar electrode attached to an electrical stimulator (Myopacer Field Simulator, 10N, IonOptix, Westwood, MA, http://www.ionoptix.com) was used to electrically pace monolayers at 0.5 Hz. In separate experiments, responsiveness to isoproterenol (50 nmol/l) was evaluated 45 days after cardiac induction in 96-well plates. Briefly, monolayers were loaded with Rhod-2 (100 μl/well, Molecular Probes) in dimethyl sulfoxide at 37°C for 20 minutes. Spontaneous beating rate, calcium transient amplitude, and duration were quantified before and after isoproterenol treatment.

Statistical Analysis

Quantitative data analyses were performed in triplicate and presented as the mean $\pm$ SD. The data were analyzed by Student's *t* test or analysis of variance with Bonferroni correction for multiple comparisons using GraphPad Prism software (version 6.0e, GraphPad, La Jolla, CA, http://www.graphpad.com). Results were considered to be statistically significant if $p \leq .05$, unless otherwise stated.

RESULTS

Human AF-MSCs Have Restricted Differentiation Potential

We isolated human AF-MSCs in the absence of cell sorting and confirmed their phenotype after several weeks in culture. In comparison with spindle-shaped neonatal dermal fibroblasts grown in

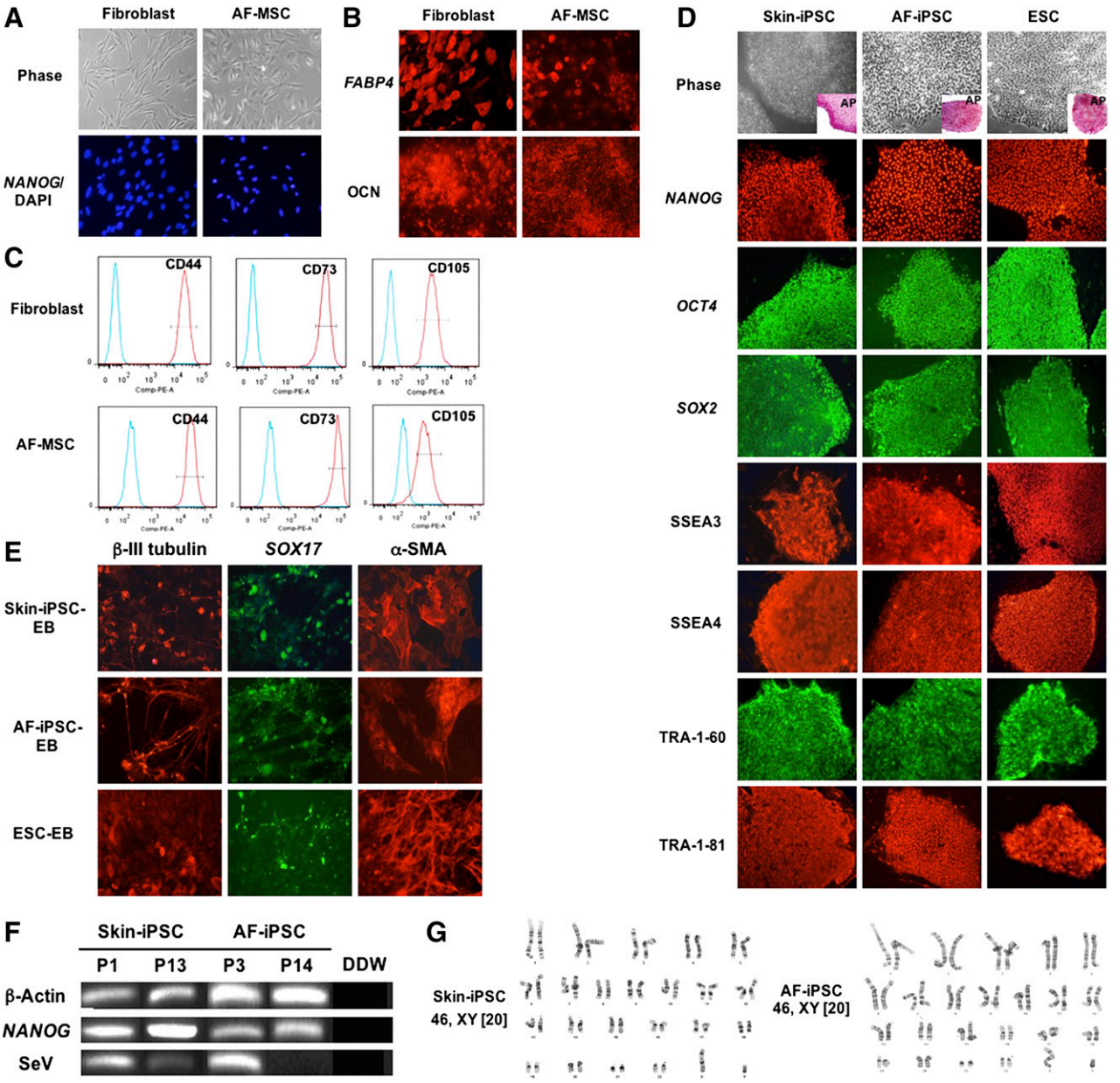

Figure 1. Characterization of human amniotic fluid mesenchymal stromal cells (AF-MSCs) before and after cellular reprogramming with non-integrating Sendai virus (SeV, passage 4, magnification, ×10). Human skin dermal fibroblasts were reprogrammed in parallel experiments as controls. **(A):** Representative phase contrast photomicrographs illustrating the typical morphology of skin and amniotic fluid cells (upper panels). Immunofluorescence microscopy of cells merged with 4′,6-diamidino-2-phenylindole (in blue) showing lack of expression of the pluripotency marker, NANOG, in both cell types (lower panels). **(B):** Immunofluorescence microscopy of representative mesenchymal skin and amniotic fluid cells under adipogenic conditions showing expression of adipogenic marker, fatty acid binding protein 4 (upper panels, magnification, ×40). Immunofluorescence microscopy of representative mesenchymal skin and amniotic fluid cells under osteogenic conditions demonstrating expression of osteogenic marker, osteocalcin (lower panels, magnification, ×40). **(C):** Flow cytometric characterization of representative skin dermal fibroblasts and AF-MSCs (positive shown in red in comparison with blue negative control) grown in mesenchymal basal media, confirming a mesenchymal stromal immunophenotypic profile. **(D):** Representative colony morphology, alkaline phosphatase staining (inset), and immunofluorescence profile of skin- and amniotic fluid (AF)-induced pluripotent stem cells (iPSCs) showing similarities with human embryonic stem cell (ESC) controls (magnification, ×20). **(E):** Immunofluorescence microscopy of representative adherent embryoid bodies from skin-iPSCs, AF-iPSCs, and ESCs showing spontaneous three-germ layer expression of β-III tubulin (ectoderm), *SOX17* (endoderm), and α-smooth muscle actin (mesoderm), magnification, ×20. **(F):** Representative reverse transcription polymerase chain reaction from skin- and AF-iPSC clones demonstrating maintenance of *NANOG* but loss of SeV transgene sequences at later passages. Double distilled water was a negative control. **(G):** Representative karyotype analysis of skin- and AF-iPSC colonies based on 20 G-banded metaphase cells, indicating normal chromosomes (passage 17). Abbreviations: AF-MSC, amniotic fluid mesenchymal stromal cells; AP, alkaline phosphatase; DAPI, 4′,6-diamidino-2-phenylindole; DDW, double distilled water; EB, embryoid bodies; ESC, embryonic stem cell; FABP4, fatty acid binding protein 4; iPSC, amniotic fluid-induced pluripotent stem cells; OCN, osteocalcin; SeV, Sendai virus; α-SMA, alpha-smooth muscle actin.

parallel, the majority of amniocytes had a more distinct, oval-shaped morphology after the first passage (Fig. 1A). As was expected, immunofluorescent staining showed lack of expression of the pluripotency marker, *NANOG*, in both cell types (Fig. 1A). AF-MSCs were successfully maintained in continuous culture for 4 weeks ($\approx 3.7 \times 10^7$ cells at passage 4) without morphologic change or reduced cell proliferation.

To characterize the baseline differentiation potential of unsorted AF-MSCs, we performed directed differentiation toward the mesodermal lineage. We confirmed that a subset of AF-MSCs were capable of differentiating into two mesodermal cell types, adipocytes and osteoblasts, when cultured in the appropriate directive media for 3 weeks. Evidence of adipogenic differentiation was indicated by the presence of Oil Red O-positive lipid vacuoles within the cytoplasm of a subpopulation of AF-MSCs (data not shown) and by expression of fatty acid binding protein 4 (Fig. 1B) by immunofluorescence. There was osteogenic differentiation, as evidenced by increased extracellular calcium matrix staining in the presence of Alizarin Red (data not shown) and by positive expression of the late osteogenic marker, *OCN* (Fig. 1B).

The immunophenotypic profile of AF-MSCs was further characterized by flow cytometry. Both AF-MSCs and dermal fibroblasts uniformly expressed surface epitope markers typically associated with bone marrow-derived mesenchymal stromal cells (Fig. 1C). For AF-MSCs and dermal fibroblasts, expression of CD44 was 98.9% $\pm$ 1.4% and 97.3% $\pm$ 2.5%, CD73 was 91.9% $\pm$ 4.5% and 99.5% $\pm$ 0.4%, CD90 was 94.9% $\pm$ 5.3% and 95.9% $\pm$ 3.1%, and CD105 was 95.6% $\pm$ 3.5% and 98.3 $\pm$ 2.1%, respectively. In contrast, less than 1% of all samples expressed HLA-DR or stem cell markers, including CD34, CD45, *NANOG*, and *OCT4A*. The expression of CD117 among AF-MSCs was uniformly low (0.9% $\pm$ 0.1%; data not shown).

Reliable Reprogramming of Amniocytes Using SeV Vectors

To epigenetically reprogram AF-MSCs into transgene-free iPSCs, we used nonintegrating SeV allowing for controlled overexpression of OSKM. Under standard ESC conditions, AF-MSCs uniformly began to aggregate while reducing cytoplasmic volume and losing their spindle-shaped morphology between 14 and 21 days in culture (Fig. 1D). After 28 days, there were multiple candidate iPSC colonies with well-defined borders and high nuclear-to-cytoplasm ratios analogous to undifferentiated ESCs. We confirmed that morphologically distinct AF-iPSCs expressed high levels of alkaline phosphatase (Fig. 1D, inset). The overall reprogramming efficiency of AF-MSCs into iPSCs using SeV encoding for OSKM ranged from 0.01% to 0.05%.

Between four and six weeks after exposure to SeV reprogramming factors, individual AF-iPSC clones were mechanically picked and successfully transferred onto Matrigel-coated dishes for further expansion, subculture, and additional characterization. Immunofluorescence staining revealed uniformly high expression of *NANOG, OCT4, SOX2*, SSEA3, SSEA4, TRA-1-60, and TRA-1-81 within AF-iPSC colonies in a pattern similar to that seen with dermal skin-iPSCs and ESC colonies (Fig. 1D).

To confirm that AF-iPSCs were capable of trilineage differentiation in vitro, we allowed clones to spontaneously differentiate in low-adherence cultures as EBs. Whereas AF-MSCs had neither the ability to form EBs nor the capability of surviving in suspension, AF-iPSCs exhibited robust EB formation. Immunocytochemical analysis of AF-iPSC-EBs confirmed the presence of derivatives of three germ layers similar to EBs generated from skin-iPSCs and ESCs. AF-iPSC-EBs expressed the endoderm markers, *SOX17* (Fig. 1E) and *FOXA2* (data not shown). Mesodermal differentiation was confirmed by the presence of α-SMA (Fig. 1E), and ectodermal differentiation was exhibited by positive β-III tubulin (Fig. 1E) and Nestin (data not shown) expression.

Evidence of residual genomic integration of SeV vectors in iPSCs was evaluated by RT-PCR. As expected, there was strong expression of the pluripotency marker, *NANOG*, among all AF-iPSC and skin-iPSC clones at later passages. In contrast, levels of the SeV transgene were nearly undetectable beyond passage 10 (Fig. 1F). Cytogenetic analyses showed normal karyotypes, indicating that AF-iPSCs remained free of nonclonal aberrations after continuous in vitro expansion for up to passage 20 (Fig. 1G).

Transgene-Free Amniocytes Could Be Reliably Induced Toward the Cardiac Lineage

We subjected six different AF-iPSC clones to cardiogenic conditions by using either the Matrigel sandwich (n = 3 experiments) or small-molecule (n = 1 experiment) protocol. Schematic diagrams of CM differentiation are shown in Figure 2A and 2B, respectively. Between 7 and 10 days after induction, amniotic fluid-derived cells began to spontaneously contract, consistent with CM differentiation. Cardiac induction was reliably achieved with similar efficiency from all clones using either differentiation protocol. Over time, the majority of cells continued to beat in a coordinated, rhythmic fashion (mean frequency, 100.8 $\pm$ 16.2 beats per minute at 37.5 days; supplemental online video), and spontaneously contracting cells could be maintained in culture for at least 90 days. Immunofluorescence staining approximately 4 weeks after induction showed strong expression within contracting cells of *MYH7*, α-actinin, and MF20, in a pattern similar to that observed with skin-CMs and ESC-CMs, which confirmed directed differentiation of transgene-free AF-iPSCs into functional CMs (Fig. 2C). Over time, there was alignment and increased density of myofilaments within individual AF-CMs, as displayed by robust immunofluorescence staining for α-actinin and cTnT (Fig. 2D). We could maintain AF-CMs under these cardiogenic conditions for at least 90 days.

Qualitative gene expression analyses of transgene-free AF-CMs performed between 30 and 60 days after cardiac induction showed upregulation of multiple CM-specific genes (Fig. 2E), namely *MYH6, MYH7, TNNT2,* MLC2a (*MYL7*), MLC2v (*MYL2*), and *TTN*, in AF- and skin-CMs, in comparison with controls when normalized in relation to the housekeeping gene, *GAPDH*. Gene expression of *MYH7, TNNT2*, MLC2a, MLC2v, and *TTN* was significantly increased in AF-CMs in comparison with skin-CM controls. As was expected, pluripotency genes, including *NANOG, OCT4, SOX2*, and *TERT*, were uniformly downregulated in AF- and skin-CMs after induction in comparison with parental controls (Fig. 2E). Taken together, these results are consistent with differentiation of stem cells to functional CMs.

AF-CMs Are Composed of Multiple Cardiac Subtypes

To obtain a more homogeneous population of transgene-free CMs for subsequent phenotypic characterization and functional testing, both AF-CMs and skin-CMs were enriched on the basis

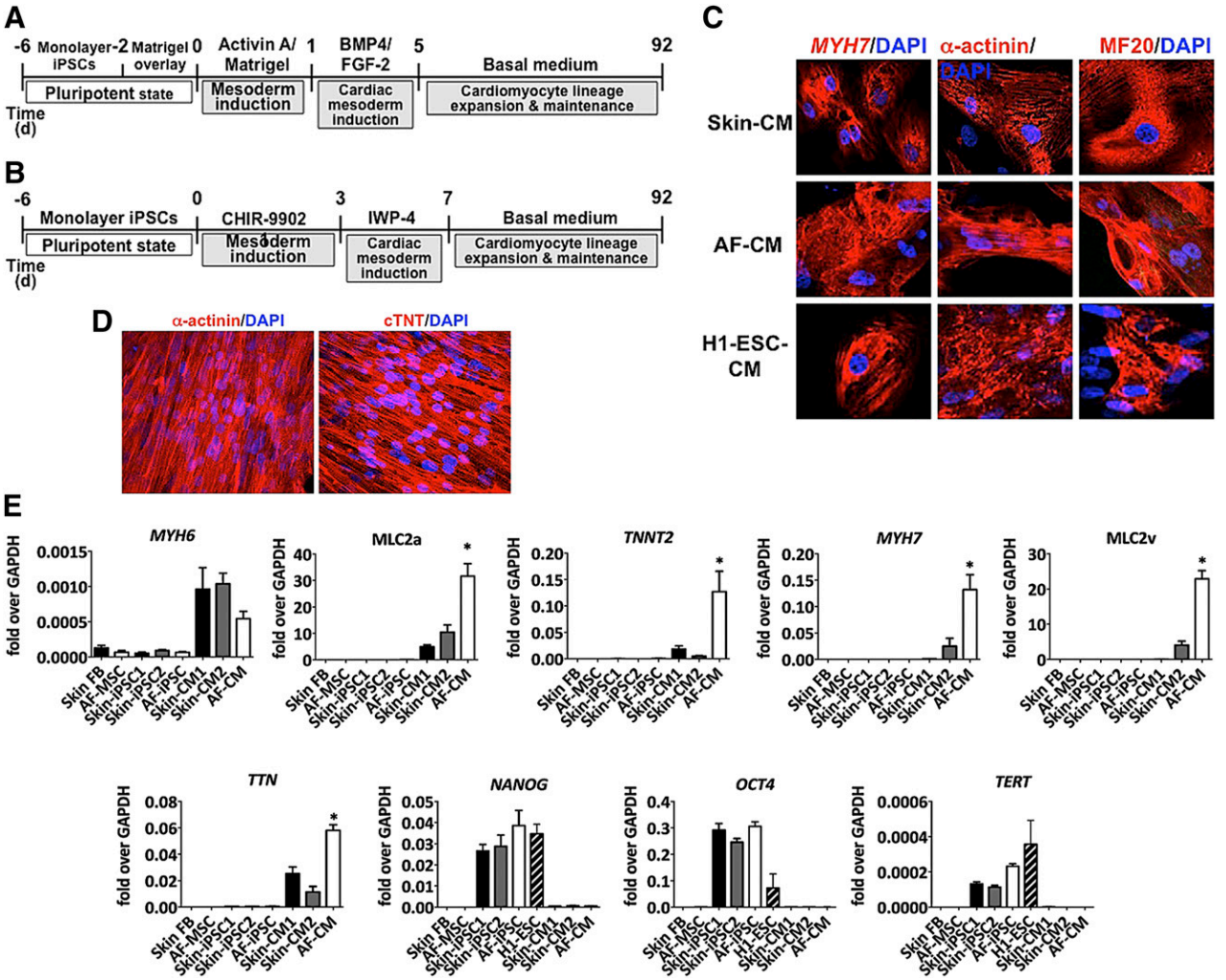

Figure 2. Directed differentiation of representative transgene-free amniotic fluid-induced pluripotent stem cells (iPSC) clones from amniotic fluid into cardiomyocytes (CMs) in vitro. **(A):** Schematic of Matrigel sandwich CM induction (n = 3 separate experiments). **(B):** Schematic of small-molecule CM induction (n = 1 experiment). **(C):** Skin- and amniotic fluid-derived cardiomyocytes (AF-CMs) at day 38 of induction revealing positive immunofluorescent staining for myocyte markers (Cy3 secondary, red), including *MYH7*, α-actinin, and MF20 (magnification, ×40), merged with DAPI, compared with embryonic stem cell (ESC) controls. **(D):** Immunofluorescence staining of AF-CMs at day 90 using antibodies against α-actinin and cardiac troponin (Cy3 secondary, red) showing densely aligned and well-organized myofilament structures superimposed with DAPI (magnification, ×40). **(E):** Quantitative analysis by quantitative polymerase chain reaction , demonstrating marked upregulation of cardiac-specific genes—including *MYH6, MYL7* (MLC2a), *TNNT2, MYH7, MYL2* (MLC2v), and *TTN*—in skin- and AF-CMs after 42 days of induction in comparison with skin fibroblast (FB) and amniotic fluid controls. Gene expression of *MYH7, TNNT2, MYL7, MYL2,* and *TTN* was significantly increased in AF-CMs in comparison with skin-CM controls. Pluripotency genes—such as *NANOG, OCT4,* and *TERT*—were downregulated. Data were normalized in relation to housekeeping gene (*GAPDH*) and presented as the mean ± SEM. *, $p \leq .05$ in comparison with skin-CMs; n = 3 independent biological replicates. Abbreviations: AF-CMs, amniotic fluid-derived cardiomyocytes; BMP4, bone morphogenetic protein 4; CMs, cardiomyocytes; DAPI, 4′,6-diamidino-2-phenylindole; ESC, embryonic stem cell; FB, fibroblast; iPSC, amniotic fluid-induced pluripotent stem cells; MSC, mesenchymal stem cell.

of SIRPA$^+$ expression between 30 and 40 days after induction. In comparison with unsorted cells whose SIRPA expression was between 53.2% and 65.3%, greater than 90% enrichment for SIRPA was obtained in all samples after magnetic bead separation (Fig. 3A). CM purity for AF-CMs and skin-CMs, as determined by flow cytometry based on cTnT expression, was 96.8% ± 0.83% and 93.2% ± 2.68%, respectively. There were no significant differences in cTnT expression between AF-CMs and skin-CMs after sorting (p = .057). To determine the degree of hypertrophy among sorted cells, we measured relative cell size and found it to be, on average, 68% greater in AF-CMs than in skin-CMs (p = .029, Fig. 3B). Confocal microscopy of AF- and skin-CMs showed multiple CM subtypes on the basis of immunostaining for various sarcomeric proteins, including *MLC2v*, *MYH7*, MF20, MLC2a, and *TNNT2* (Fig. 3C).

To accurately determine the relative frequency of atrial- and ventricular-like CMs derived from SIRPA$^+$ AF-CMs, we measured MLC2a and MLC2v promoter activity driving green fluorescent protein (GFP) expression for more than 24 hours. As is shown by GFP cell imaging (Fig. 3D), there was proliferation and relatively stable MLC2a- and MLC2v-GFP expression among AF-CMs in a similar profile when compared with skin-CMs. There were no

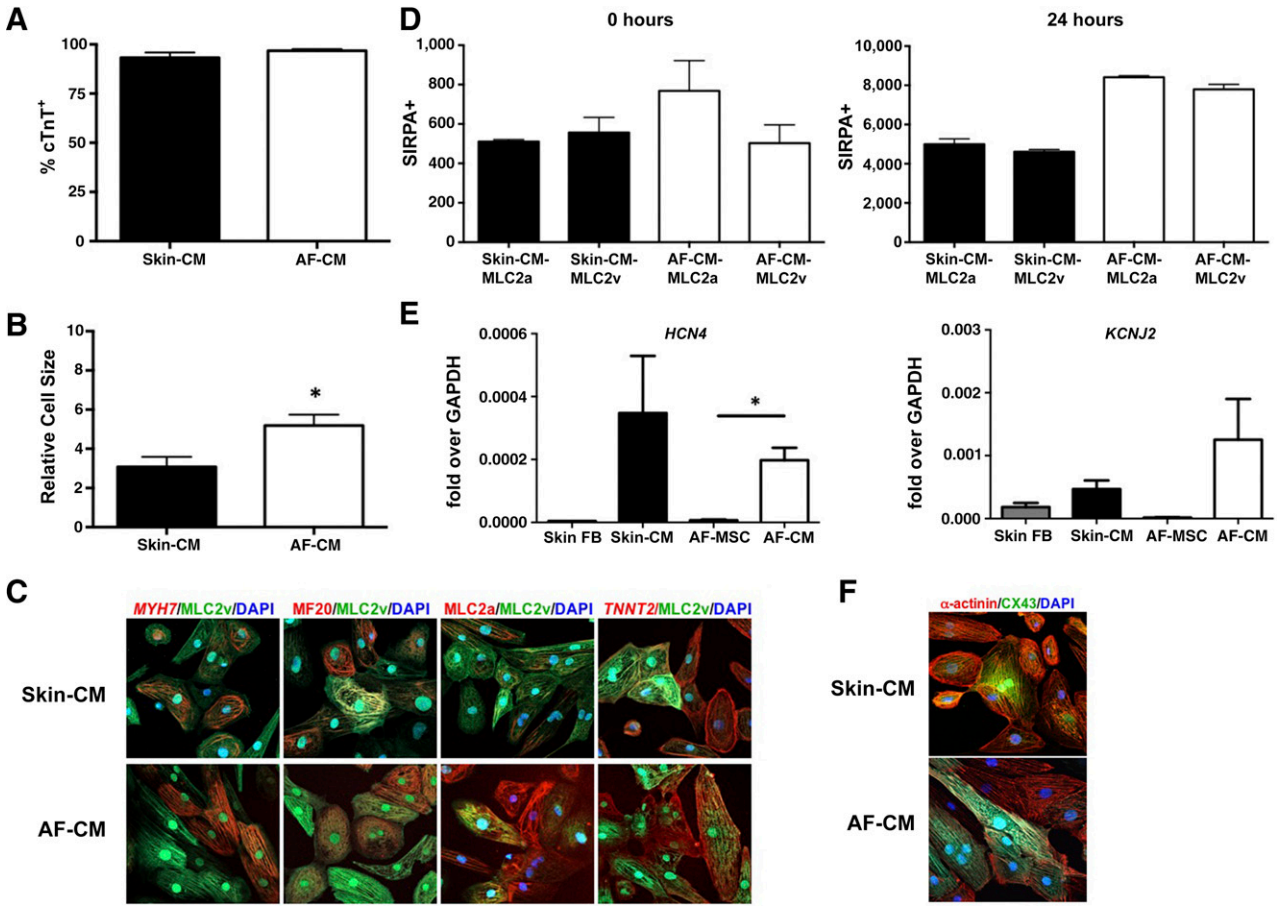

Figure 3. Characteristics of transgene-free amniotic fluid-derived cardiomyocytes (AF-CMs) at induction day 38, $n = 3$ independent biological replicates. **(A):** Vertical bar graph showing high enrichment for cardiac troponin cells in both skin-CMs (93.2% ± 1.3%, black) and AF-CMs (96.8% ± 0.4%, white) after positive selection based on signal regulatory protein (SIRPA) expression. Data are presented as mean ± SD, $n = 3$ independent biological replicates. **(B):** Vertical bar graph demonstrating a significant increase in the relative size of AF-CMs in comparison with skin-CMs (3.1 ± 0.3, black) and AF-CMs (5.2 ± 0.3, white). Data are presented as mean ± SD. ∗, $p \leq .05$ in comparison with control, $n = 3$ independent biological replicates. **(C):** Confocal microscopy of skin- and AF-CM subtypes exhibiting comparable mixed immunostaining patterns of sarcromeric proteins, including ventricular CMs (myosin light chain 2v [MLC2v], fluorescein isothiocyanate [FITC] secondary, green) in conjunction with other cardiac-specific markers, including *MYH7, MF20*, MLC2a, and *TTNT2*. Nuclei were counterstained in DAPI in all images. **(D):** Quantification of SIRPA$^+$ CM subtypes at 0 hours (left) and 24 hours (right) in culture showing relatively stable MLC2a- and MLC2v-green fluorescent protein (GFP) expression among skin-CMs (black) and AF-CMs (white). Data are presented as mean ± SD, $n = 4$ independent biological replicates. **(E):** Quantitative gene expression analysis by quantitative polymerase chain reaction demonstrating upregulation of cardiac-specific membrane channel genes, including *HCN4* (sinoatrial node, top) and *KCNJ2* (inwardly rectifying potassium channel, bottom), in skin- and AF-CMs in comparison with control parental cells. Data were normalized in relation to the housekeeping gene (*GAPDH*) and presented as the mean ± SD. ∗, $p \leq .05$ in comparison with control, $n = 3$ independent biological replicates. **(F):** Confocal microscopy of skin- and AF-CMs demonstrating expression of the gap junction protein, connexin-43 (CX43, FITC secondary, green), in conjunction with the microfilament protein, α-actinin (Cy3 secondary, red). Nuclei were counterstained with DAPI. Abbreviations: AF-CMs, amniotic fluid-derived cardiomyocytes; cTnT, cardiac troponin cells; DAPI, 4′,6-diamidino-2-phenylindole; FB, fibroblast; MLC2, myosin light chain 2; MSC, mesenchymal stem cell; SIRPA, signal regulatory protein.

significant differences between atrial- and ventricular-like specification of AF-CMs at 24 hours (52.7% and 47.3%, respectively). To further characterize the presence of nodal-like subtypes within AF-CMs, we measured the gene expression of *HCN4*, an important membrane channel specific for the sinoatrial node (Fig. 3E). *HCN4* expression was strongly upregulated after cardiac differentiation in AF-CMs, similar to skin-CMs, when compared with control parental cells. There was also marked upregulation in the *KCNJ2*, a gene encoding for an inwardly rectifying potassium channel, in AF-CMs, similar to expression observed in skin-CM controls. Finally, confocal microscopy of AF-CMs showed expression of the critical gap junction protein, connexin-43 (*GJA1*), in conjunction with the microfilament protein, α-actinin.

Global Gene Expression of AF-CMs Is Similar to That of Skin-CMs

To determine any similarities and differences between AF-CMs and skin-CMs, we tested iPSC clones with parental somatic cells and SIRPA$^+$ CMs (induction day 31) in targeted microarray analyses. A representative dendrogram of one-way unsupervised hierarchicial clustering analysis of global expression profiles showed that AF-iPSCs clustered closely with skin-iPSCs (Fig. 4A). Both iPSCs were distinct from parental AF-MSCs and clustered remotely with dermal fibroblasts (Fig. 4A). Although global gene expression patterns of AF-iPSCs were divergent from those of AF-MSCs ($R^2 = .58$) and AF-CMs ($R^2 = .28$), AF-CMs arrays were

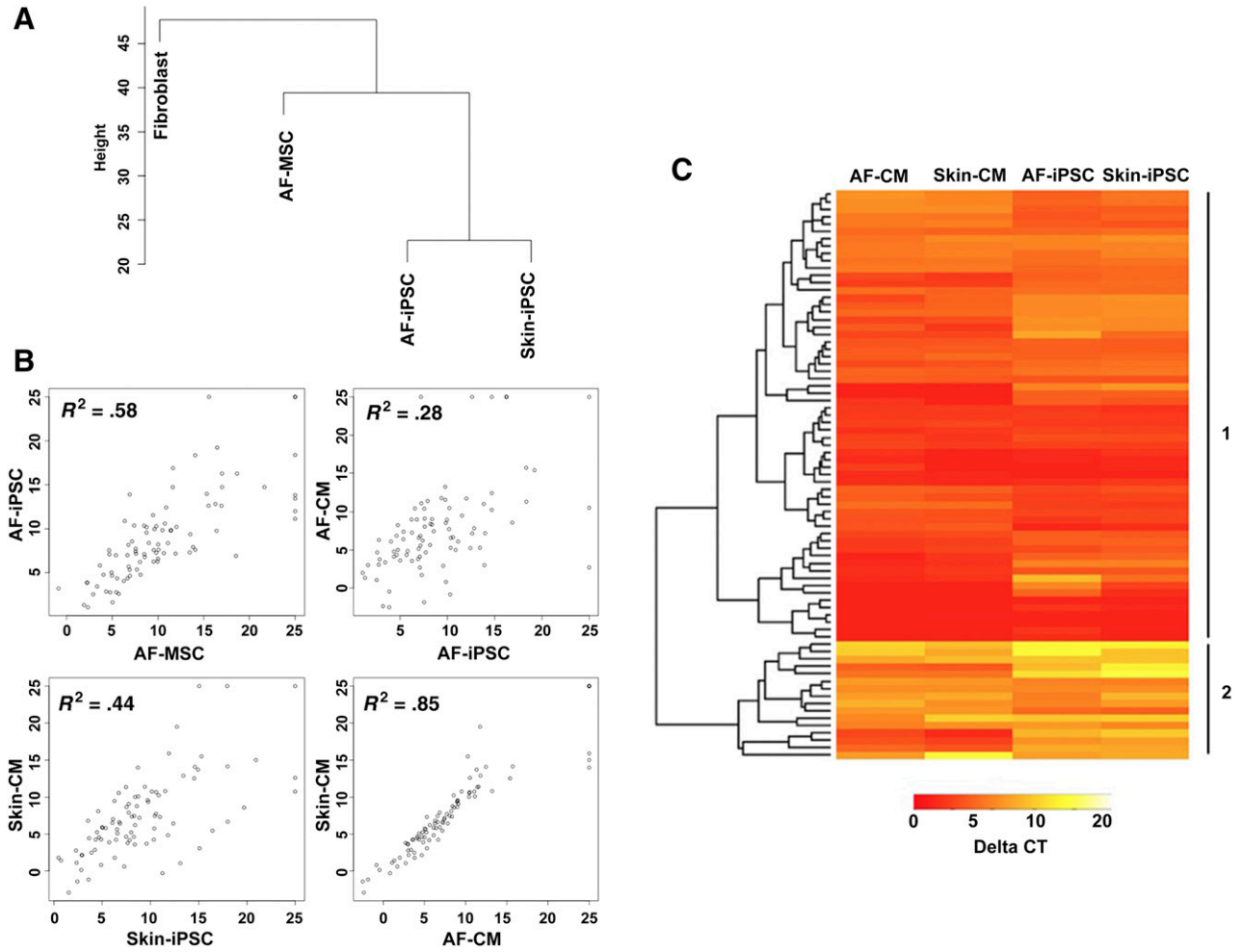

Figure 4. Representative microarray analysis of transgene-free signal regulatory protein amniotic fluid-derived cardiomyocytes (AF-CMs) (induction day 31) in comparison with controls, n = 2 independent biological replicates. **(A):** Dendrogram showing the unsupervised hierarchal clustering of the global expression profiles for amniotic fluid-induced pluripotent stem cells (AF-iPSCs), parental AF-mesenchymal stem cell (MSC), skin-iPSCs, and dermal fibroblasts. **(B):** Global gene expression profiles of AF-CMs shown in scatter plots revealing close correlation with patterns observed in skin-CMs (R^2 = .85, bottom right) in comparison with parental AF-iPSCs (R^2 = .28, top right). R^2 denotes the coefficient of determination. **(C):** Heatmap image illustrating the relationship of 88 genes, grouped on the basis of hierarchical clustering, which were differentially upregulated or downregulated in AF-CMs, skin-CMs, AF-MSCs, and dermal fibroblasts. The transcriptome patterns expressed by AF-CMs were similar to those expressed by skin-CMs. Higher and lower levels of transcripts are shown in red and yellow, respectively. Listings of genes in group 1 and group 2 are presented in supplemental online Tables 3 and 4, respectively. GEO link: http://www.ncbi.nlm.nih.gov/geo/query/acc.cgi?acc = GSE76965. Abbreviations: AF-MSC, amniotic fluid mesenchymal stem cell; CMs, cardiomyocytes; iPSC, amniotic fluid-induced pluripotent stem cells.

closely aligned with patterns observed in skin-CMs (R^2 = .85; Fig. 4B). To assess the similarities and differences between CMs in more detail, a heatmap focusing on upregulated and downregulated genes was generated, which revealed transcriptome patterns in AF-CMs that were nearly identical to those found in skin-CMs (Fig. 4C). In accordance with the qPCR data, focused analysis of key sarcomere structural genes—including *ACTC1*, *MYH6*, and *NEBL*—showed upregulation in both AF-CMs and skin-CMs with no significant differences between the groups.

AF-CMs Demonstrate Robust Functional Activity

The spontaneous beat rate of representative CMs from iPSCs was measured by counting spontaneous calcium transients. There were no significant differences in the beat rate per minute between skin- and AF-CMs when measured early after induction on day 21 (12.3 ± 5.5 vs. 21.5 ± 9.9) or day 28 (38.9 ± 14.2 vs. 26.0 ± 10.9, respectively; Fig. 5A).

Between days 38 and 45 after induction, SIRPA$^+$ AF-CMs underwent functional testing in parallel with SIRPA$^+$ skin-CMs as controls. AF-CMs had a significantly faster mean spontaneous beat rate of 73.8 ± 5.4 beats per minute (frequency of 1.23 ± 0.09, n = 15) in comparison with skin-CMs (mean 48.6 ± 3.6 beats per minute, 0.81 ± 0.06 Hz, n = 9). To further investigate the functional properties of AF-CMs, we measured calcium handling properties by using fluorescent imaging techniques. Line scan plots and single pixel recordings made during 5-second intervals showed that AF-CMs exhibited a spontaneous rhythmic frequency and timing comparable to those of control skin-CMs (Fig. 5B, 5C, respectively). We then conducted optical mapping studies to measure the wave propagation characteristics of AF-CMs and found isotropic propagation patterns of intracellular

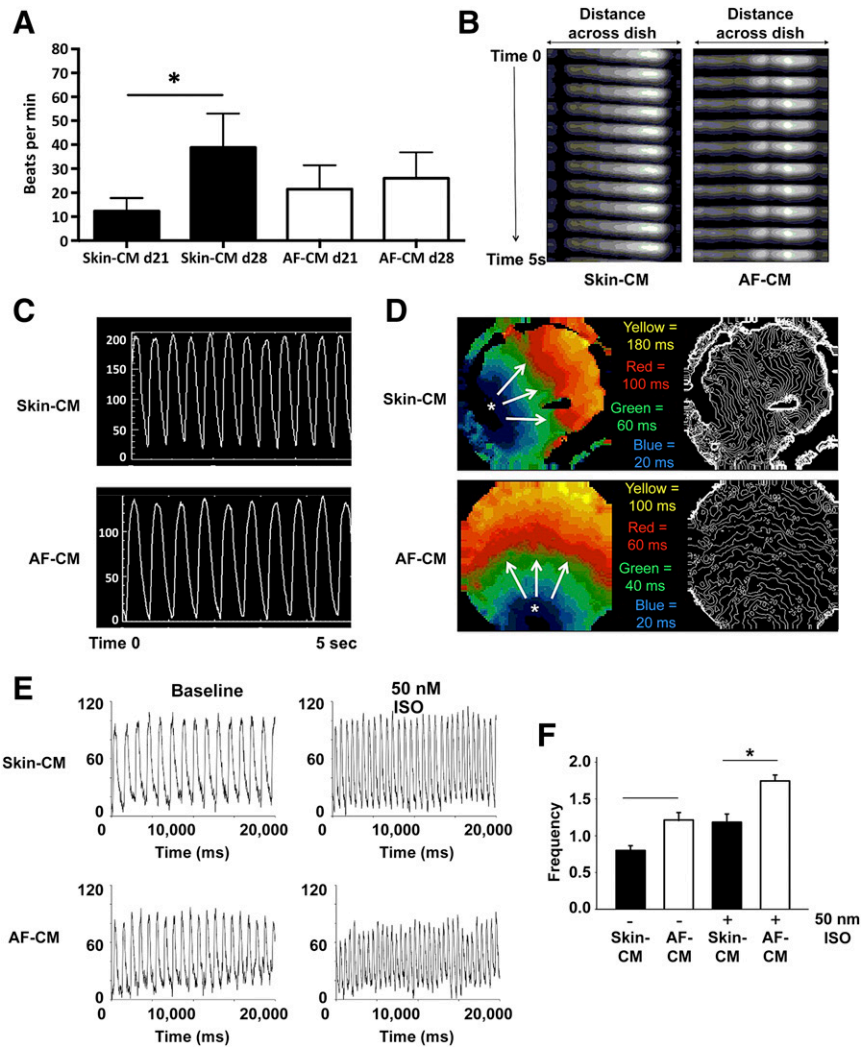

Figure 5. Functional characterization of transgene-free amniotic fluid-derived cardiomyocytes (AF-CMs). **(A):** Spontaneous beat rate per minute of representative CMs derived from skin and amniotic fluid at day 21 and day 28 after cardiac induction. $*$, $p \leq .05$. **(B):** Representative line scan images of signal regulatory protein ($SIRPA^+$) CMs derived from skin (left) and amniotic fluid (right) during a 5-second interval. **(C):** Representative single-pixel recordings of $SIRPA^+$ skin- and AF-CMs during a 5-second interval. **(D):** Representative pseudocolor activation map of intracellular calcium transient propagation in $SIRPA^+$ skin-CM (top) and AF-CM (bottom) monolayers showing similar circular spreading patterns after spontaneous activation. Isochrone lines indicate differential activation times. **(E):** Representative calcium transient recordings after β-adrenergic agonist (50 nM isoproterenol [ISO]) exposure of $SIRPA^+$ skin- and AF-CMs demonstrating appropriate chronotropic responses in comparison with baseline. **(F):** Measurement of baseline frequencies revealing faster spontaneous beat rate among representative $SIRPA^+$ AF-CMs ($n = 15$) in comparison with skin-CMs ($n = 9$). Recordings after 50 nM ISO exposure of skin- and AF-CMs, demonstrating an increase in beat frequencies. $*$, $p \leq .05$ in comparison with control. Abbreviations: AF-CMs, amniotic fluid-derived cardiomyocytes; d21, day 21; ISO, isoproterenol.

calcium transients in AF-CM monolayers that were similar to those observed in skin-CMs (Fig. 5D). To further analyze calcium handling properties in response to β-adrenergic receptor stimulation, we exposed AF-CMs to isoproterenol (50 nM). AF-CMs demonstrated appropriate chronotropic responses, as shown by a statistically significant increase in the beat frequency in comparison with baseline and stimulated skin-CMs ($p = .008$; Fig. 5E, 5F). Taken together, AF-CMs electrically matured in monolayer cultures in similar fashion to those observed with skin-CMs.

Discussion

Our laboratory has previously shown that transgene-free iPSCs can be generated from somatic cells derived from amniotic fluid samples from normal and abnormal pregnancies [10]. Although the generation of iPSCs from amniotic fluid has been well documented by multiple groups [19–22], there remains little to no data on their systematic differentiation potential toward the CM lineage [23]. In this study, we show that human amniotic fluid cells with restricted differentiation potential can be reprogrammed using nonintegrating SeV and subsequently used to generate functional CMs with robust and highly organized myofilament structures. We also demonstrate that a diverse population of relatively mature CMs was produced, expressing MLC2v, MLC2a, and *TNNT2*, among others transcripts. The majority of these cells expressed SIRPA, which is present on human fetal CMs as well as on iPSC-derived CMs from the earliest cardiac stage [14]. Given that our data showed that $SIRPA^+$ AF-CMs responded appropriately to pharmacologic stimulation, these studies suggest that we may have an in vitro platform for the testing of other agents, including

morphogens and growth factors, which have the potential to enhance early CM function, differentiation, or both.

The entire process from a 10-ml amniotic fluid sampling to transgene-free CM generation took fewer than 16 weeks (i.e., 2–3 weeks for AF-MSC culture, 6–8 weeks for iPSC colony formation and expansion, and approximately 3–4 weeks for CM differentiation), using a highly reproducible protocol in all six iPSC clones tested. In most cases of prenatally diagnosed CHD, AF-CMs could be available for personalized application, including in vitro testing and autologous transplant-based therapies, at the time of their initial palliative heart surgical reconstruction as neonates. Use of more defined cardiac differentiation protocols, including those using small molecules as shown in our study, strengthens the notion that the generation of AF-CMs is not protocol specific. Our findings are consistent with the work of others showing that CMs derived from dermal fibroblasts using small molecules have indistinguishable cardiac phenotypic and calcium-handling properties when compared with those generated using the Matrigel sandwich technique [24]. The small-molecule approach may further reduce concerns regarding the safety of these cells when delivered for therapeutic purposes [25]. More rapid generation of AF-CMs by direct differentiation of somatic cells may also be possible in the near future on the basis of reports documented elsewhere [26, 27].

Our highly enriched AF-CMs were essentially indistinguishable from those derived from dermal fibroblasts. While postnatal dermal fibroblasts will likely remain the somatic cell of choice for basic cardiac research aimed at mechanistically dissecting the processes involved in cardiac differentiation from iPSCs, the generation of CMs for therapeutic purposes in prenatally diagnosed CHD favors the use of autologous amniocytes as the parental cell of choice [28]. Moreover, amniocytes offer numerous advantages over postnatal cells, because the former proliferate more rapidly, may be easier to reprogram toward pluripotency, are more responsive to directed differentiation, and harbor few to no spontaneous genetic aberrations [21, 29, 30].

Because most major fetal cardiac anomalies are initially diagnosed between 20 weeks and 24 weeks gestation [31], generating CMs from amniotic fluid would be the least invasive strategy for facilitating both early in vitro testing and effective stem cell therapy in either the prenatal or postnatal period. At 24 weeks gestation, from a volume of amniotic fluid of approximately 600 ml surrounding the fetus [32], a 10-ml aliquot obtained by amniocentesis avoids the inherent risk of hemorrhage, preterm labor, and fetal demise associated with a fetal skin or placenta biopsy [7]. An amniocentesis also has virtually no added morbidity because it is often a recommended test conducted in the prenatal workup of a major cardiac anomaly to rule out an abnormal karyotype [33]. Furthermore, our group, among others [34], has previously shown that amniotic fluid cells can be harvested without maternal cell contamination and are therefore derived exclusively from the fetus [10]. The traditional paradigm of creating autologous cardiac tissues from postnatal tissue may lead to undesirable delays in therapy and potentially poorer outcomes in those with severe CHD [28].

The differentiation of human embryonic and other fetal stem cell derivatives into CMs has also been proposed for potential clinical translation in pediatric cardiac disease [35]. Options would include "off-the-shelf" stem cell products, such as $CD117^+$ amniotic fluid stem cells (AFSCs), dermal fibroblast-derived iPSCs, and ESCs [36–38]. Although these alternative cells types are attractive for many reasons and would offer some potential advantages clinically, they are hampered by other issues, including possible immunologic rejection due to major and minor major histocompatibility differences [38]. Moreover, concerns regarding inadvertent tumor formation with ESCs and many iPSCs when injected in vivo have limited enthusiasm for their clinical translation potential [39]. Finally, ethical objections to the use of human ESC-based therapies in the United States and elsewhere on the basis of religious/social norms should not be underestimated [40].

Most critical CHD—including tetralogy of Fallot, transposition of the great vessels, and hypoplastic left heart syndrome (HLHS)—are complex structural problems resulting from poorly understood global errors in cardiac morphogenesis. Unlike hypertrophic cardiomyopathy and congenital arrhythmias, both of which have been shown to recapitulate the disease phenotype in iPSC models [41, 42], CM function in most critical CHD patients is believed to be intrinsically normal in the majority of cases, suggesting that most cases of CHD-associated heart failure may be amenable to autologous cell therapy. Additionally, because amniotic fluid and AF-iPSCs cells can be easily banked, our approach is highly scalable and not limited by cell scarcity for most perinatal applications, including the study of 3D microtissue formation, as well as the delivery of AF-CMs to rescue heart failure or augment existing function during the initial palliative operation [35, 43–45]. Assuming that adequate proliferation of AF-iPSCs can be established and maintained in culture, this technology could also be used to seed an entire decellularized heart with CMs in time for implantation during early infancy [46]. From a 10-ml aliquot of amniotic fluid, at least 1.35×10^7 $cTnT^+$ cells could be easily generated before birth by using our highly scalable approach. On the basis of clinical translation studies performed by others [47–49], approximately $2–4 \times 10^7$ CMs would be required to extensively remuscularize the damaged heart of a 3-kg neonate with congenital heart disease.

Unlike endogenous resident CM progenitors isolated from heart biopsies [50, 51], the study of amniotic fluid-based iPSCs would additionally allow investigators to identify genes and molecular regulatory networks that mediate early CM differentiation and morphogenesis in any prenatally diagnosed patient. For HLHS and other forms of critical CHD, this in vitro platform would be ideally suited to study patient-specific developmental defects that may lead to differences in myocardial patterning [52]. Although somatic mutations in *NKx2-5, NOTCH1, GATA4,* and *HAND1* have been implicated in the pathogenesis of CHD [53, 54], other investigators have not been able to substantiate these findings [6, 55]. Because the cause is largely unknown in the vast majority of critical CHD, it is likely that no single gene defect is specifically linked in most cases of CHD.

Novel insights into disease pathogenesis may also be gained using this AF-iPSC-based cardiac differentiation protocol in terms of understanding the role of resident, $SIRPA^-$ non-CMs, which likely include vascular smooth muscle cells, fibroblasts, and endothelial cells that are vital in supporting normal CM development within 3D microtissues [56]. Moreover, the study of AF-CMs from critical CHD amniotic fluid within bioreactors could be used to explore how aberrant physiologic conditions in utero (e.g., hypoxia, laminar flow, stretch, compression) affect CM differentiation [51].

In our study, the isolated cells from amniotic fluid had a phenotype that was consistent with that of MSCs [8, 57]. Because these AF-MSCs had an intermediate phenotype between that

of true pluripotent stem cells and fully differentiated adult stromal cells [58–60], our amniocytes should not be confused with $CD117^+$ AFSCs [37]. Although both AF-MSCs and AFSCs proliferate easily in culture, our group, among others, has shown that AF-MSCs undergo senescence following repetitive passaging, are not pluripotent, and cannot be differentiated directly into CMs using established protocols [60]. In contrast, AFSCs have been elegantly shown to be pluripotent on the basis of a transgene-free, chemical-based approach using the histone deacetylase inhibitor, valproic acid [61]. However, because a rare ($<1\%$) clonal population of $CD117^+$ amniotic fluid cells must be isolated and cultured for months, their use for autologous purposes at birth may not be feasible [62]. It is also not entirely clear as to whether $CD117^+$ cells are reliably present in every amniotic fluid specimen [63], particularly during the time period when critical CHD is typically diagnosed by fetal echocardiography (i.e., between 20 and 24 weeks gestation) [64].

Despite the promising data generated from this study, there are some limitations. iPSC reprogramming of any somatic cell using SeV is still a technically demanding endeavor, and multiple passages were required before loss of the SeV transgene was evident. Although AF-CMs displayed similar behavior as did skin-CMs, comparisons with additional control CMs that were directly derived from human fetal/neonatal cardiac tissue would be ideal to better understand their relative behavior and efficacy in clinical applications. Our CM differentiation protocols will also require further modifications prior to preclinical and clinical use, because they are neither completely chemically defined nor free from animal products. Recently, other investigators have made significant progress in establishing fully chemically defined differentiation and xenogeneic-free protocols for the generation of CMs [25]. There may also be variations in the differentiation capabilities of various iPSC clones, which is beyond the scope of our study. Finally, evaluation of additional patient samples, particularly from fetuses with prenatally diagnosed CHD, would be highly desirable because, to our knowledge, iPSC-based technologies have not been described in nonsyndromic cases of major structural CHD. Experiments in the laboratory are currently focusing on transgene-free AF-CMs generated from patients with HLHS and other various forms of critical CHD.

Conclusion

The present study demonstrates that cells from second-trimester human amniotic fluid can be reliably reprogrammed and induced into mature, functional CMs free of reprogramming factors. Because most critical CHD can be detected in utero, this approach has the potential to generate patient-specific, therapeutic-grade CMs amenable for autologous cell transplantation before a child is even born.

Acknowledgments

This work was supported by the Robert Wood Johnson Foundation Harold Amos Award and by institutional start-up funds provided by the Department of Surgery, University of Michigan. We thank Jeannie Kreutzman, M.S.N., C.P.N.P., for facilitating the collection of amniotic fluid specimens, as well as Craig Johnson and Christopher Krebs for their assistance with the microarray analysis.

Author Contributions

G.J.: conception and design, collection and/or assembly of data, performance of in vitro experiments, data analysis and interpretation, manuscript writing; T.J.H.: conception and design, analysis and interpretation of electrophysiology data, manuscript editing; J.D.B.: collection and/or assembly of data, data analysis and interpretation; K.A.W.: data analysis and interpretation, manuscript editing; K.S.O.: conception and design, financial support, manuscript editing; S.M.K.: conception and design, provision of study material or patients, data analysis and interpretation, manuscript writing, manuscript editing, final approval of manuscript.

Disclosure of Potential Conflicts of Interest

The authors indicated no potential conflicts of interest.

References

1 Oster ME, Lee KA, Honein MA et al. Temporal trends in survival among infants with critical congenital heart defects. Pediatrics 2013; 131:e1502–e1508.

2 Quartermain MD, Pasquali SK, Hill KD et al. Variation in prenatal diagnosis of congenital heart disease in infants. Pediatrics 2015;136: e378–e385.

3 Feinstein JA, Benson DW, Dubin AM et al. Hypoplastic left heart syndrome: Current considerations and expectations. J Am Coll Cardiol 2012;59(Suppl):S1–S42.

4 Haase A, Olmer R, Schwanke K et al. Generation of induced pluripotent stem cells from human cord blood. Cell Stem Cell 2009;5: 434–441.

5 Shaw SW, David AL, De Coppi P. Clinical applications of prenatal and postnatal therapy using stem cells retrieved from amniotic fluid. Curr Opin Obstet Gynecol 2011;23:109–116.

6 Huang GY, Xie LJ, Linask KL et al. Evaluating the role of connexin43 in congenital heart disease: Screening for mutations in patients with outflow tract anomalies and the analysis of knock-in mouse models. J Cardiovasc Dis Res 2011;2:206–212.

7 Kunisaki SM, Armant M, Kao GS et al. Tissue engineering from human mesenchymal amniocytes: A prelude to clinical trials. J Pediatr Surg 2007;42:974–980; discussion 979–980.

8 Dominici M, Le Blanc K, Mueller I et al. Minimal criteria for defining multipotent mesenchymal stromal cells. The International Society for Cellular Therapy position statement. Cytotherapy 2006;8:315–317.

9 Bentley JK, Popova AP, Bozyk PD et al. Ovalbumin sensitization and challenge increases the number of lung cells possessing a mesenchymal stromal cell phenotype. Respir Res 2010;11:127.

10 Jiang G, Di Bernardo J, Maiden MM et al. Human transgene-free amniotic-fluid-derived induced pluripotent stem cells for autologous cell therapy. Stem Cells Dev 2014;23:2613–2625.

11 Itskovitz-Eldor J, Schuldiner M, Karsenti D et al. Differentiation of human embryonic stem cells into embryoid bodies compromising the three embryonic germ layers. Mol Med 2000;6:88–95.

12 Zhang J, Klos M, Wilson GF et al. Extracellular matrix promotes highly efficient cardiac differentiation of human pluripotent stem cells: The matrix sandwich method. Circ Res 2012; 111:1125–1136.

13 Karakikes I, Senyei GD, Hansen J et al. Small molecule-mediated directed differentiation of human embryonic stem cells toward ventricular cardiomyocytes. Stem Cells Translational Medicine 2014;3:18–31.

14 Dubois NC, Craft AM, Sharma P et al. SIRPA is a specific cell-surface marker for isolating cardiomyocytes derived from human pluripotent stem cells. Nat Biotechnol 2011;29:1011–1018.

15 Livak KJ, Schmittgen TD. Analysis of relative gene expression data using real-time quantitative PCR and the 2(-Delta Delta C(T)) method. Methods 2001;25:402–408.

16 Bizy A, Guerrero-Serna G, Hu B et al. Myosin light chain 2-based selection of human iPSC-derived early ventricular cardiac myocytes. Stem Cell Res 2013;11:1335–1347.

17 Herron TJ, Lee P, Jalife J. Optical imaging of voltage and calcium in cardiac cells & tissues. Circ Res 2012;110:609–623.

18 Lee P, Klos M, Bollensdorff C et al. Simultaneous voltage and calcium mapping of genetically

purified human induced pluripotent stem cell-derived cardiac myocyte monolayers. Circ Res 2012;110:1556–1563.

19 Ye L, Chang JC, Lin C et al. Induced pluripotent stem cells offer new approach to therapy in thalassemia and sickle cell anemia and option in prenatal diagnosis in genetic diseases. Proc Natl Acad Sci USA 2009;106:9826–9830.

20 Galende E, Karakikes I, Edelmann L et al. Amniotic fluid cells are more efficiently reprogrammed to pluripotency than adult cells. Cell Reprogram 2010;12:117–125.

21 Ginsberg M, James D, Ding BS et al. Efficient direct reprogramming of mature amniotic cells into endothelial cells by ETS factors and TGFβ suppression. Cell 2012;151:559–575.

22 Anchan RM, Quaas P, Gerami-Naini B et al. Amniocytes can serve a dual function as a source of iPS cells and feeder layers. Hum Mol Genet 2011;20:962–974.

23 Guan X, Delo DM, Atala A et al. In vitro cardiomyogenic potential of human amniotic fluid stem cells. J Tissue Eng Regen Med 2011; 5:220–228.

24 Hwang HS, Kryshtal DO, Feaster TK et al. Comparable calcium handling of human iPSC-derived cardiomyocytes generated by multiple laboratories. J Mol Cell Cardiol 2015;85:79–88.

25 Burridge PW, Matsa E, Shukla P et al. Chemically defined generation of human cardiomyocytes. Nat Methods 2014;11:855–860.

26 Jayawardena TM, Egemnazarov B, Finch EA et al. MicroRNA-mediated in vitro and in vivo direct reprogramming of cardiac fibroblasts to cardiomyocytes. Circ Res 2012;110:1465–1473.

27 Fu JD, Stone NR, Liu L et al. Direct reprogramming of human fibroblasts toward a cardiomyocyte-like state. Stem Cell Rep 2013;1:235–247.

28 Schmidt D, Mol A, Breymann C et al. Living autologous heart valves engineered from human prenatally harvested progenitors. Circulation 2006;114(Suppl):I125–I131.

29 Kaviani A, Guleserian K, Perry TE et al. Fetal tissue engineering from amniotic fluid. J Am Coll Surg 2003;196:592–597.

30 Maherali N, Hochedlinger K. Guidelines and techniques for the generation of induced pluripotent stem cells. Cell Stem Cell 2008;3: 595–605.

31 Stoll C, Garne E, Clementi M. Evaluation of prenatal diagnosis of associated congenital heart diseases by fetal ultrasonographic examination in Europe. Prenat Diagn 2001;21:243–252.

32 Brace RA, Wolf EJ. Normal amniotic fluid volume changes throughout pregnancy. Am J Obstet Gynecol 1989;161:382–388.

33 Song MS, Hu A, Dyamenahalli U et al. Extracardiac lesions and chromosomal abnormalities associated with major fetal heart defects: comparison of intrauterine, postnatal and postmortem diagnoses. Ultrasound Obstet Gynecol 2009;33:552–559.

34 In't Anker PS, Scherjon SA, Kleijburg-van der Keur C et al. Isolation of mesenchymal stem cells of fetal or maternal origin from human placenta. STEM CELLS 2004;22:1338–1345.

35 Files MD, Boucek RJ. 'Shovel-ready' applications of stem cell advances for pediatric heart disease. Curr Opin Pediatr 2012;24:577–583.

36 Laflamme MA, Chen KY, Naumova AV et al. Cardiomyocytes derived from human embryonic stem cells in pro-survival factors enhance function of infarcted rat hearts. Nat Biotechnol 2007;25:1015–1024.

37 De Coppi P, Bartsch G Jr., Siddiqui MM et al. Isolation of amniotic stem cell lines with potential for therapy. Nat Biotechnol 2007;25: 100–106.

38 Bollini S, Cheung KK, Riegler J et al. Amniotic fluid stem cells are cardioprotective following acute myocardial infarction. Stem Cells Dev 2011;20:1985–1994.

39 Cunningham JJ, Ulbright TM, Pera MF et al. Lessons from human teratomas to guide development of safe stem cell therapies. Nat Biotechnol 2012;30:849–857.

40 Nisbet M, Markowitz EM. Understanding public opinion in debates over biomedical research: looking beyond political partisanship to focus on beliefs about science and society. PLoS One 2014;9:e88473.

41 Sun N, Yazawa M, Liu J et al. Patient-specific induced pluripotent stem cells as a model for familial dilated cardiomyopathy. Sci Transl Med 2012;4:130ra47.

42 Moretti A, Bellin M, Welling A et al. Patient-specific induced pluripotent stem-cell models for long-QT syndrome. N Engl J Med 2010;363:1397–1409.

43 Kunisaki SM. Congenital anomalies: Treatment options based on amniotic fluid-derived stem cells. Organogenesis 2012;8:89–95.

44 Christoforou N, Liau B, Chakraborty S et al. Induced pluripotent stem cell-derived cardiac progenitors differentiate to cardiomyocytes and form biosynthetic tissues. PLoS One 2013;8:e65963.

45 Liau B, Christoforou N, Leong KW et al. Pluripotent stem cell-derived cardiac tissue patch with advanced structure and function. Biomaterials 2011;32:9180–9187.

46 Ott HC, Matthiesen TS, Goh SK et al. Perfusion-decellularized matrix: Using nature's platform to engineer a bioartificial heart. Nat Med 2008;14:213–221.

47 Chong JJ, Yang X, Don CW et al. Human embryonic-stem-cell-derived cardiomyocytes regenerate non-human primate hearts. Nature 2014;510:273–277.

48 Guyette JP, Charest JM, Mills RW et al. Bioengineering human myocardium on native extracellular matrix. Circ Res 2016;118:56–72.

49 Forrester JS, Price MJ, Makkar RR. Stem cell repair of infarcted myocardium: An overview for clinicians. Circulation 2003;108:1139–1145.

50 Mishra R, Vijayan K, Colletti EJ et al. Characterization and functionality of cardiac progenitor cells in congenital heart patients. Circulation 2011;123:364–373.

51 Gaber N, Gagliardi M, Patel P et al. Fetal reprogramming and senescence in hypoplastic left heart syndrome and in human pluripotent stem cells during cardiac differentiation. Am J Pathol 2013;183:720–734.

52 Jiang Y, Habibollah S, Tilgner K et al. An induced pluripotent stem cell model of hypoplastic left heart syndrome (HLHS) reveals multiple expression and functional differences in HLHS-derived cardiac myocytes. STEM CELLS TRANSLATIONAL MEDICINE 2014;3:416–423.

53 Theis JL, Hrstka SC, Evans JM et al. Compound heterozygous NOTCH1 mutations underlie impaired cardiogenesis in a patient with hypoplastic left heart syndrome. Hum Genet 2015;134:1003–1011.

54 Kobayashi J, Yoshida M, Tarui S et al. Directed differentiation of patient-specific induced pluripotent stem cells identifies the transcriptional repression and epigenetic modification of NKX2-5, HAND1, and NOTCH1 in hypoplastic left heart syndrome. PLoS One 2014;9:e102796.

55 Esposito G, Butler TL, Blue GM et al. Somatic mutations in NKX2–5, GATA4, and HAND1 are not a common cause of tetralogy of Fallot or hypoplastic left heart. Am J Med Genet A 2011;155A:2416–2421.

56 Bani D, Formigli L, Gherghiceanu M et al. Telocytes as supporting cells for myocardial tissue organization in developing and adult heart. J Cell Mol Med 2010;14:2531–2538.

57 In 't Anker PS, Scherjon SA, Kleijburg-van der Keur C et al. Amniotic fluid as a novel source of mesenchymal stem cells for therapeutic transplantation. Blood 2003;102:1548–1549.

58 Evangelista M, Soncini M, Parolini O. Placenta-derived stem cells: New hope for cell therapy? Cytotechnology 2008;58:33–42.

59 Lee JM, Jung J, Lee HJ et al. Comparison of immunomodulatory effects of placenta mesenchymal stem cells with bone marrow and adipose mesenchymal stem cells. Int Immunopharmacol 2012;13:219–224.

60 Connell JP, Ruano R, Jacot JG. Amniotic fluid-derived stem cells demonstrate limited cardiac differentiation following small molecule-based modulation of Wnt signaling pathway. Biomed Mater 2015;10:034103.

61 Moschidou D, Mukherjee S, Blundell MP et al. Valproic acid confers functional pluripotency to human amniotic fluid stem cells in a transgene-free approach. Mol Ther 2012;20:1953–1967.

62 Diecke S, Wu JC. Pushing the reset button: Chemical-induced conversion of amniotic fluid stem cells into a pluripotent state. Mol Ther 2012;20:1839–1841.

63 Zia S, Toelen J, Mori da Cunha M et al. Routine clonal expansion of mesenchymal stem cells derived from amniotic fluid for perinatal applications. Prenat Diagn 2013;33:921–928.

64 Moschidou D, Mukherjee S, Blundell MP et al. Human mid-trimester amniotic fluid stem cells cultured under embryonic stem cell conditions with valproic acid acquire pluripotent characteristics. Stem Cells Dev 2013;22:444–458.

See www.StemCellsTM.com for supporting information available online.